

# 1 Transformation of Ferrite Proeutectoid Carbon during Cooling of Super Long-Rang-Zhang Suo-Quan(张所全)<sup>a,b</sup>, Jiao Si-Hai(焦四海)<sup>b</sup>, Ding

Jian-Hua(丁建华)<sup>b</sup>,

Wan Di(万迪)<sup>c</sup>, Liu Zhen-Yu(刘振宇)<sup>a</sup>, Wang Guo-Dong(王国栋)<sup>a</sup>

<sup>a</sup>State Key Laboratory of Rolling and Automation, Northeastern University, Shenyang 110004, Liaoning, China;

<sup>b</sup>Research Institute, Baoshan Iron & Steel Co., Ltd., Shanghai 201900, China;

<sup>c</sup>Department of Mechanical and Industrial Engineering, Norwegian University of Science and Technology, Richard Birkelands vei 2B, NO-7491 Trondheim, Norway

**Abstract:** In order to explore the possible diffusion distance of carbon during proeutectoid ferrite transformation, a slow cooling test of low carbon steel was carried out under vacuum of the thermal simulator. The microstructure and thermal expansion curve were discussed, the carbon concentration inside the sample was measured. The ferrite layer of about 450  $\mu\text{m}$  thickness was obtained without pearlite on the surface of the sample in the microstructure. The thermal expansion curve shows that the ferrite layer without pearlite is formed during the local phase transformation, which is followed by the global transformation. The carbon concentration in the core of the sample (0.061%) is significantly higher than that of the bulk material (0.054%). All results show that carbon has long-range diffusion from the outer layer to the inner layer of the sample. The transformation is predominantly interface-controlled mode during local transformation, and the interface migration rate is about 2.25  $\mu\text{m/s}$ .

**Keywords:** low carbon steel; local transformation; super long rang diffusion; interface-controlled mode.

## 1 Introduction

During the proeutectoid ferrite transformation from austenite, two kinds of diffusion will occur. The first one is the carbon diffusion in ferrite and austenite, which is highly temperature dependent [1-5]. The solubility of carbon in ferrite is about two orders of magnitude smaller than

---

**Foundation date:** Project (16PJ1430200) supported by Shanghai Pujiang Program

**Received date:** 0000-00-00; **Accepted date:** 0000-00-00

**Corresponding author:** (ZHANG Suo-quan, M. A.; Senior Engineer; Tel: +86-21-26645939; E-mail: zhangsuoquan@baosteel.com)

1  
2  
3 that in austenite, therefore the carbon atoms will segregate to the interphase boundaries in  
4 austenite if they can't diffuse into austenite matrix in time. The exact magnitude of accumulation  
5 depends on the diffusion velocity of carbon in austenite [6]. Carbon can diffuse through one or  
6 more austenite grains, and thus it is called long-range diffusion. The other one is the diffusion of  
7 matrix atoms, and this diffusion realizes the phase transformation from a face-centered cubic (f.c.c)  
8 symmetry (austenite) into a body-centered cubic (b.c.c) symmetry (ferrite). This process also  
9 causes the movement of the  $\gamma \rightarrow \alpha$  interface into the austenite matrix. In this case, the Fe atoms  
10 move only to the adjacent positions, which is called short-range diffusion. The above-mentioned  
11 two kinds of diffusion occur between the newly formed ferrite and the adjacent austenite grains.  
12  
13  
14  
15  
16  
17

18 Over the past several decades, there have been a number of models describing the kinetics of  
19 proeutectoid ferrite transformation. In many of them, the proeutectoid ferrite transformation is  
20 assumed to develop under local equilibrium conditions. In this case, the carbon concentration at  
21 interface is equal to the  $\gamma$ - $\alpha$  equilibrium concentration; the rate of transformation from f.c.c lattice  
22 to b.c.c lattice is extremely fast; and the kinetics of proeutectoid ferrite transformation is  
23 considered to be diffusion-controlled [7-12]. Another extreme is called interface-controlled. In this  
24 situation, there is no carbon concentration gradient in austenite. The kinetics is reflected by  
25 interface mobility, which was defined by Christian [13]. Actually, both the interface mobility and  
26 the diffusivity of carbon in austenite are finite, and thus the mixed-mode character was adopted to  
27 describe the proeutectoid ferrite transformation. Nolfi et al. [14] investigated the mixed-mode  
28 character when they described the dissolution and growth of spherical precipitates. Extensive  
29 studies on mixed-mode models have been performed by Krielaart et al. [15-22]. Kop [17] also  
30 modeled the transformation in terms of interface mobility. Using hot stage transmission electron  
31 microscopy, an in-situ study of austenite decomposition was realized by Onink et al. [23], this  
32 experiment showed the phenomena occurring near the transformation interface during the  
33 austenite to ferrite transformation, and directly measured the interface migration rates. In the  
34 studies above, the ferrite nucleation is considered to occur homogeneously in all parts of the  
35 specimen, both on the surface and in the core. The diffusion of carbon only occurs between the  
36 newly-formed ferrite and adjacent austenite. Super long-range diffusion of carbon during  
37 proeutectoid ferrite transformation has not been mentioned.  
38  
39  
40  
41  
42  
43  
44  
45  
46  
47

48 The novelty of this work lies in realizing the super long-range carbon diffusion. The  
49 proeutectoid ferrite layer of about 450  $\mu\text{m}$  thickness was obtained in this study due to the carbon  
50 diffusion from the surface into the interior of the specimen. Based on the results, a new process  
51 has been developed, which can achieve varying microstructure for the surface and interior of  
52 specimen. For example, ferrite microstructure with good plasticity was obtained on the surface,  
53 and the microstructure of ferrite plus bainite with high strength was obtained in the core part of the  
54 specimen. In this way, a better combination of formability and strength was obtained for some  
55 bending or twisting workpieces. This work will be introduced in a following paper. This study just  
56  
57  
58  
59  
60

focuses on the realization of the super long-range diffusion of carbon.

## 2 Experimental

### 2.1 Experimental material

The compositions of the studied steel is listed in Table 1. To ensure easy diffusion of carbon, a low carbon steel with high Tr3 was selected. Cylindrical ingot was cast in a vacuum induction furnace in laboratory. After forging and hot rolling, a plate with thickness of 30 mm was quenched to room temperature to ensure a more homogeneous distribution of carbon. Cylindrical specimens with a diameter of 8 mm and a height of 12 mm were machined from the quenched plate.

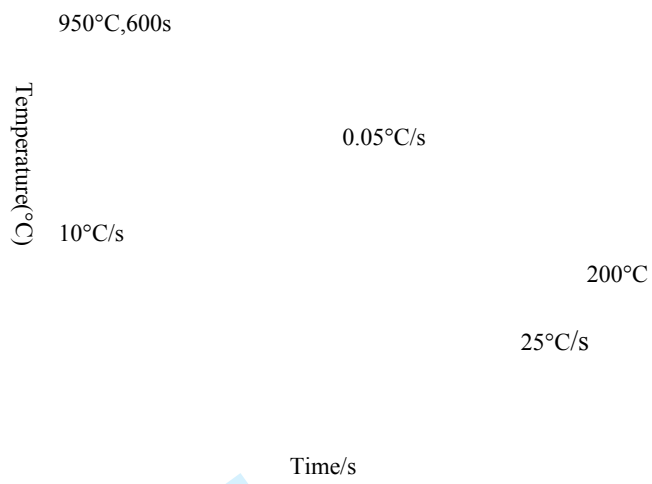
**Table 1** Chemical compositions(weight percent) of the studied steel

	C	Si	Mn	P	S	Fe
wt.%	0.05400	0.26338	0.51176	0.00540	0.00228	Bal.

### 2.2 Experimental method

The slow cooling test was realized in the thermal simulated test machine (DSI MAXSTRAIN-20). Under the vacuum condition of less than 0.12 torr pressure, the sample was heated to 950 °C at a heating rate of 10 °C/s. Austenitization took place at this temperature for 600s, after which the sample was slowly cooled down to 200 °C at a cooling rate of 0.05 °C/s, and subsequently cooled down to room temperature at a cooling rate of 25 °C/s. The cooling rate was rather low to ensure that carbon has adequate time to diffuse when temperature is slightly lower than Tr3. The time, temperature and thermal expansion curves were automatically recorded by the thermal simulator. Fig.1 illustrates the process of the slow cooling test.

1  
2  
3  
4  
5  
6  
7  
8  
9  
10  
11  
12  
13  
14  
15  
16  
17  
18  
19  
20  
21  
22  
23  
24  
25  
26  
27  
28  
29  
30  
31  
32  
33  
34  
35  
36  
37  
38  
39  
40  
41  
42  
43  
44  
45  
46  
47  
48  
49  
50  
51  
52  
53  
54  
55  
56  
57  
58  
59  
60



For Review Only

Fig.1 Schematic drawing of the slow cooling test.

The sample after cooling test was evenly divided into two parts along the center of the height. One of the new surfaces was polished and etched with 4% nital solution (volume fraction). The microstructure of the sample was observed by optical microscope.

To prove the carbon diffusion from the outer layer of the specimen into the interior of specimen, the carbon concentration inside the sample was measured. The material from the outer layer of the cylindrical sample was removed with a reduction in the diameter from 8 mm to 6.8 mm, and the height was changed from 12 mm to 8 mm, as is shown in Fig.2. The material of the smaller cylindrical specimen was machined into drillings, and then the carbon concentration was measured with the carbon sulfur analyzer (Leco CS-444LS USA).

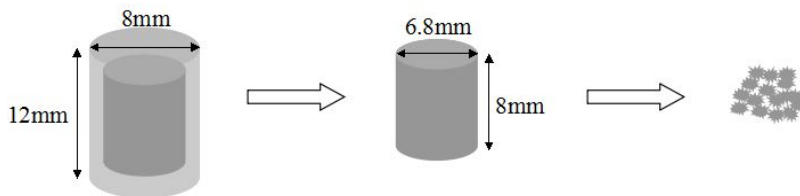
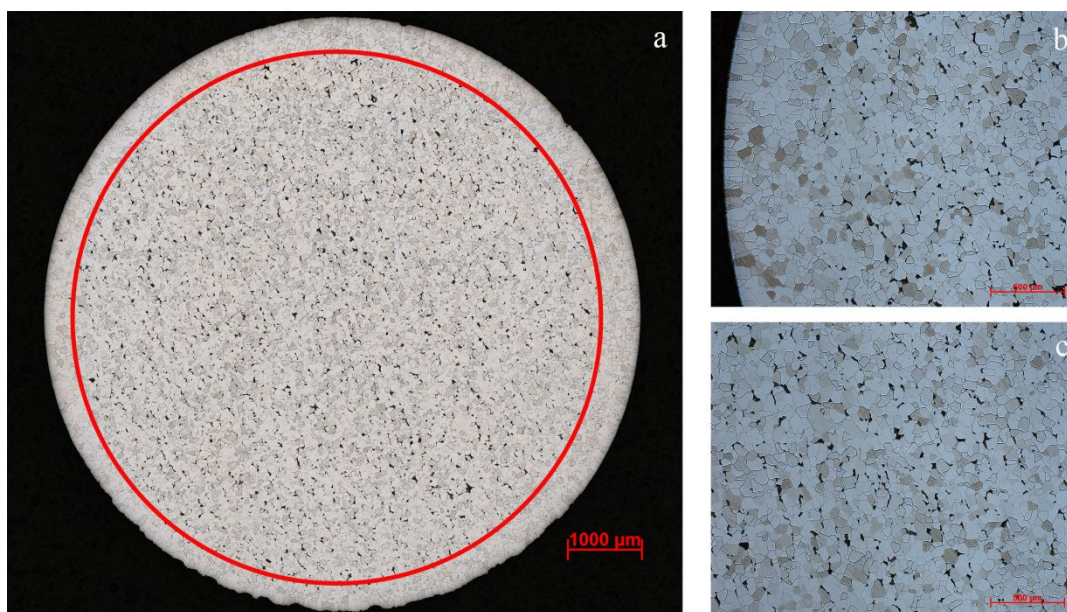


Fig.2 Schematic drawing of the drillings preparation

### 3 Results and discussion

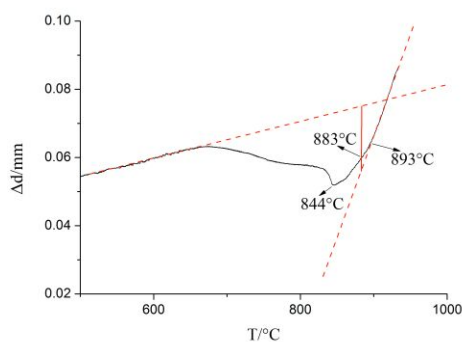
#### 3.1 Experiment results

Fig.3 shows the microstructure of the investigated specimen. It can be seen that the microstructure can be divided into two different regions by the highlighted red circle in Fig.3a. The outer white bright layer has an unevenly distributed thickness varying from 400  $\mu\text{m}$  to 550  $\mu\text{m}$ , in which only proeutectoid ferrite can be observed. Fig.3b shows the magnified surface region with the transition from ferrite near the surface to a mixed phase of ferrite and pearlite in the interior. Fig.3c shows the homogeneously mixed phase of ferrite and pearlite in the interior of the specimen.



**Fig.3.** The microstructures after slow cooling test (a)of the whole section,  
(b)of the specimen surface, (c) of the interior.

The thermal expansion curve was recorded in real time by the thermal simulator, as shown in Fig.4. From the holding temperature to 893 °C, the diameter of the sample decreased linearly with the decrease of temperature due to no transformation occurring at this stage. Then the temperature continued to decrease, and the expansion curve began to deviate, which means that ferrite transformation started at 893 °C. Then, the thermal expansion curve deviated from the dashed line more and more, indicating that more austenite transformed into ferrite. Finally, the thermal expansion curve rose noticeably when the temperature was lower than 844 °C, which demonstrated that the effect of phase transformation expansion surpassed the effect of cooling shrinkage.



**Fig.4.** The thermal expansion curve of the slow cooling process. Ferrite transformation started at 893 °C. Diameter of specimen increased at 844 °C. Local transformation ended at 883 °C, which was calculated on the base of

microstructures and lever rule.

It is assumed that the carbon concentration of the proeutectoid ferrite (with tertiary cementite at room temperature) in the outer layer of the sample is 0.02%, which is the highest solubility of the proeutectoid ferrite at 723 ° C. The average thickness of the outer layer is 0.45 mm. If the spare carbon atoms diffused from the outer layer into the inside of cylindrical specimen, the calculated average carbon concentration of the inside of cylindrical specimen should be 0.063%. The actual measured result of the carbon concentration of drillings is 0.061%, which is lower than the calculated carbon concentration, but is significantly higher than that of the bulk material (0.054%) This is the direct evidence of the diffusion of carbon from the outer layer to the interior.

### 3.2 Discussion

Based on the theory of mixed-controlled mode [15, 18], The transformation changes from interface-controlled mode to diffusion-controlled mode due to the variation of carbon concentration distribution in austenite, as shown in Fig.5.

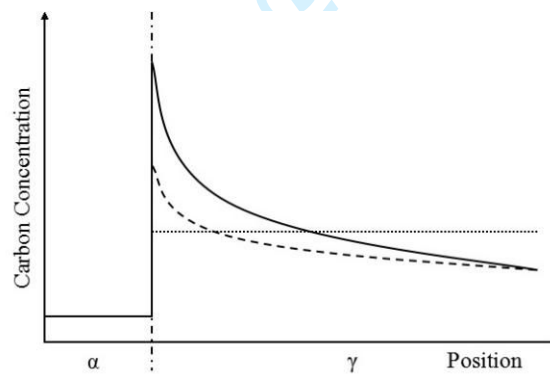


**Fig.5.** Schematic carbon concentration profiles at the ferrite-austenite interface. The dotted line gives the profile for interface-controlled mode, the dashed line for mixed-mode, and the solid line for diffusion-controlled mode, according to Krielaart [16].

In the slow cooling test, the specimen was gradually cooled from the outer layer to the interior<sup>[24]</sup>. The thermal conductivity of the steel is the lowest at the temperature of Ar3. It is more beneficial to form a temperature gradient. When both the surface temperature and the interior temperature are higher than Ar3, the microstructure remains austenite, as shown in Fig.6a. At this stage, the austenite volume shrinks with the decreasing temperature without phase transformation.

Thus, the thermal expansion curve decreases linearly with the decrease of temperature.

At a moment of slow cooling, the surface temperature of the specimen becomes lower than  $A_{r3}$  and ferrite will nucleate on the surface of specimen, while the internal structure remains austenite due to the higher temperature, as the microstructure in Fig.6b. Because of the low solubility of carbon in ferrite, the carbon atoms will diffuse from ferrite into austenite with the growth of ferrite, which means the carbon atoms will migrate from surface of the specimen to the interior. Since carbon diffusion is heavily temperature dependent, it is assumed that the concentration of carbon inside the austenite phase remains homogeneous at this stage when the temperature is high enough, as shown by the dotted line in Fig.5. The increased carbon concentration of austenite inside the specimen further reduced the transformation driving force, which makes the internal austenite more stable. At this stage, the phase transformation is interface-controlled mode. Phase transformation takes place only on the surface and does not occur in the interior of the sample, therefore it is defined as “local transformation”. With the growth of ferrite close to the surface, the thickness of ferrite layer increases gradually. Fig.3 shows that about 11.25% of the austenite in diameter direction has transformed into ferrite, based on the lever rule, the ending temperature for local transformation should be 883 °C, as indicated by the arrow in Fig.4.

Since the transformation mode here is interface-controlled, the interface migration rate depends on the corresponding driving force and the interface mobility. The driving force for interface migration is a function of carbon concentration and temperature, and the interface mobility is determined by the coherency of interface, solute drag, pinning effects, etc., thus the interface migration rate varies during the local transformation. According to the thermal expansion curve, the cooling rate of this experiment was 0.05 °C/s, and the local transformation lasted occurred from 893 °C to 883 °C, resulting in a time interval of 200 s. With the migration path of about 450  $\mu\text{m}$  measured from Fig.1, the average interface migration rate can be estimated to be 2.25  $\mu\text{m/s}$ .

When the temperature of the central specimen is lower than  $A_{r3}$ , as indicated by the dashed line in Fig.6, ferrite nucleation will occur at the grain boundary of austenite in the interior, as the microstructure in Fig.6c. From this time on, the ferrite transformation begins in the whole sample. The transformation is thus defined as “global transformation” at this stage. At the beginning of global transformation, the carbon concentration at the interface is close to the average value of the specimen and almost keeps homogeneous in austenite, so the transformation is also interface-controlled. Because of lower temperature and higher ferrite volume ratio than that of local transformation, the diffusion of carbon in austenite becomes more difficult, and carbon will accumulate at the interface. The corresponding carbon concentration profile is given by the dashed line in Fig.5. The transformation becomes mixed-mode, and the interface migration becomes slower. When the carbon concentration at the interface reaches equilibrium, as shown by the solid



line in Fig.5, the interface stops migrating, and the ferrite grains stop growing until the carbon concentration at the interface becomes lower than the equilibrium value again.

Finally, a further cooling below Ar1 leads to a transformation from the remaining austenite inside the specimen to pearlite, and the temperature profile is given by the solid line in Fig.6. Fig.6d shows the schematic of the resulting microstructure.

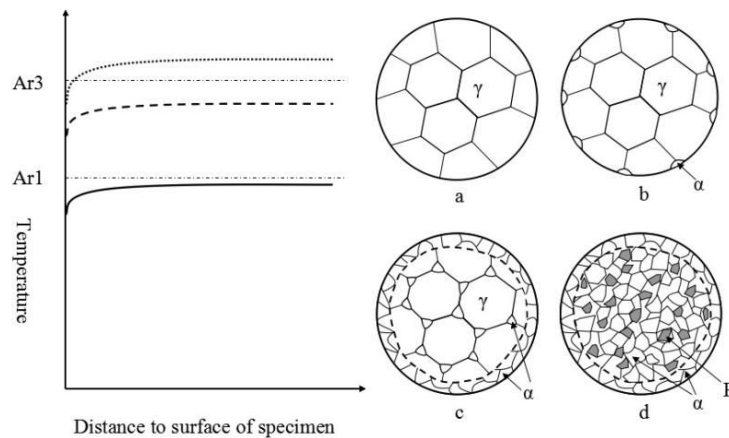


**Fig.6.** Schematic of temperature profile and microstructure development during the slow cooling test. The resulting microstructure is shown for temperature (a) above Ar3, (b) following the dotted line, (c) following the dashed line and (d) following the solid line.

#### 4 Conclusions

From the above results, the following conclusions could be drawn:

- (1) In the slow cooling test of a low carbon steel, two stages of transformation including local transformation and global transformation took place. The ferrite layer of 450  $\mu\text{m}$  thickness was obtained on the surface of the sample during the local transformation.
- (2) The measured carbon concentration in the interior specimen shows that carbon on the surface of a sample has a super long-range diffusion, and the diffusion distance should be greater than the thickness of the ferrite layer.
- (3) In the local transformation, the phase transformation mode is interface-controlled, and the interface migration rate is about 2.25  $\mu\text{m/s}$ .

#### Acknowledgement

The authors thank Dr. Aiwen Zhang, Dr. Xiaojun Liang and Dr. Xiangqian Yuan for helpful discussions, Mr. Guobin Song and Mr. Ledo Miao for their support in experiment, Research team under Dr. Sihai Jiao for financing this study.

## References

- [1] J. Ågren, Computer simulations of the austenite/ferrite diffusional transformations in low alloyed steels[J]. *Acta Metallurgica*. 30(4) (1982) 841-851.
- [2] J. Ågren, A revised expression for the diffusivity of carbon in binary Fe-C austenite[J]. *Scripta Metallurgica*. 20(11) (1986) 1507-1510.
- [3] D. Jiang, E.A. Carter, Carbon dissolution and diffusion in ferrite and austenite from first principles[J]. *Physical Review B* 67(21) (2003) 214103.
- [4] Xia Changqing, Jin Zhanpeng. Examination of carbon diffusion in niobium clad steel composite[J]. *Journal of Central South University of Technology*. 6(1)(1999) 1-3.
- [5] ZHANG Xing, TANG Jin-yuan, ZHANG Xue-rui, An optimized hardness model for carburizing-quenching of low carbon alloy steel[J]. *Journal of Central south University*. 24 (1) (2017) 9-16.
- [6] Z.-K. Liu, Theoretic calculation of ferrite growth in supersaturated austenite in Fe-C alloy[J]. *Acta Materialia*. 44(9) (1996) 3855-3867.
- [7] H. Bhadeshia, L.-E. Svensson, B. Grefott, A model for the development of microstructure in low-alloy steel (Fe-Mn-Si-C) weld deposits[J]. *Acta Metallurgica*. 33(7) (1985) 1271-1283.
- [8] M. Enomoto, Prediction of TTT-diagram of proeutectoid ferrite reaction in iron-alloys from diffusion growth theory [J]. *ISIJ International*. 32(3) (1992) 297-305.
- [9] R. Reed, H. Bhadeshia, Kinetics of reconstructive austenite to ferrite transformation in low alloy steels[J]. *Materials Science and Technology*. 8(5) (1992) 421-436.
- [10] R. Vandermeer, Modeling diffusional growth during austenite decomposition to ferrite in polycrystalline Fe-C alloys[J]. *Acta Metallurgica et Materialia*. 38(12) (1990) 2461-2470.
- [11] YE Jian-song, CHANG Hong-bing, T. Hsu, Modeling for formation of proeutectoid ferrite in steel during continuous cooling[J]. *Journal of iron and steel research international*. 11(6) (2004) 33-36.
- [12] C. Zener, Theory of growth of spherical precipitates from solid solution[J]. *Journal of Applied Physics*. 20(10) (1949) 950-953.
- [13] J.W. Christian, The theory of transformations in metals and alloys, Pergamon, Oxford, 2002, pp. 422-479.
- [14] F.V. Nolfi, P.G. Shewmon, J.S. Foster, Dissolution and growth kinetics of spherical precipitates[J]. *Transactions of the Metallurgical Society of Aime*. 245(7) (1969) 1427.
- [15] G. Krielaart, S. Van der Zwaag, Simulations of pro-eutectoid ferrite formation using a mixed

- control growth model[J]. *Materials Science and Engineering. A* 246(1-2) (1998) 104-116.
- [16] G.P. Krielaart, J. Sietsma, S. van der Zwaag, Ferrite formation in Fe-C alloys during austenite decomposition under nonequilibrium interface conditions[J]. *Materials Science and Engineering. A* 237(2) (1997) 216-223.
- [17] K. TA, Y. Van Leeuwen, J. Sietsma, S. Van Der Zwaag, Modelling the austenite to ferrite phase transformation in low carbon steels in terms of the interface mobility[J]. *ISIJ International*. 40(7) (2000) 713-718.
- [18] Y. Van Leeuwen, T. Kop, J. Sietsma, S. van der Zwaag, *J. Phys. IV France* 9(PR9) (1999) Pr9-401-Pr9-409.
- [19] Y. van Leeuwen, J. Sietsma, S. van der Zwaag, The influence of carbon diffusion on the character of the gamma-alpha phase transformation in steel [J]. *ISIJ International*. 43(5) (2003) 767-773.
- [20] Y. van Leeuwen, S. Vooijs, J. Sietsma, S. Van Der Zwaag, The effect of geometrical assumptions in modeling solid-state transformation kinetics[J]. *Metallurgical and Materials Transactions A*. 29(12) (1998) 2925-2931.
- [21] J. Sietsma, S. van der Zwaag, A concise model for mixed-mode phase transformations in the solid state[J]. *Acta Materialia*. 52(14) (2004) 4143-4152.
- [22] WU Rui-heng, RUAN Xue-yu, ZHANG Hong-bing, T.Y. Hsu, A mixed-control mechanism model of proeutectoid ferrite growth under non-equilibrium interface condition in Fe-C alloys[J]. *Journal of Materials Science & Technology*. 20(5) (2004)561-566.
- [23] M. Onink, F. Tichelaar, C. Brakman, E. Mittemeijer, S. Van Der Zwaag, An in situ hot stage transmission electron microscopy study of the decomposition of Fe-C austenites[J]. *Journal of Materials Science*. 30(24) (1995) 6223-6234.
- [24] Sobhan Mosayebidorcheh, Mohammad Rahimi-Gorji, D. D Ganji, Transient thermal behavior of radial fins of rectangular, triangular and hyperbolic profiles with temperature-dependent properties using DTM-FDM[J]. *Journal of Central South University of Technology*. 24(3)(2017) 675-682.

## 中文导读

### 先共析铁素体相变过程中碳的超长程扩散

**摘要:** 为了研究先共析铁素体相变过程中碳原子可能的扩散距离, 在热模拟的真空环境下进行了低碳钢的缓冷试验。分析了金相组织和热膨胀曲线, 同时测量了试样芯部的碳含量。在金相组织中试样的表面获得了 450 微米厚的铁素体层, 该铁素体层中不含有珠

1  
2  
3 光体。热膨胀曲线显示不含珠光体的铁素体层形成于全局相变之前的局部相变过程。试  
4 样芯部的碳含量（0.061%）显著高于基体材料的碳含量（0.054%）。所有结果显示，碳  
5 发生了从试样表层到试样芯部的超长程扩散。在局部相变过程相变主要为界面控制模式，  
6 界面迁移率大约为 2.25um/s。  
7  
8  
9

10  
11  
12 **关键词：**低碳钢；局部相变；超长程扩散；界面控制模式  
13  
14  
15  
16  
17  
18  
19  
20  
21  
22  
23  
24  
25  
26  
27  
28  
29  
30  
31  
32  
33  
34  
35  
36  
37  
38  
39  
40  
41  
42  
43  
44  
45  
46  
47  
48  
49  
50  
51  
52  
53  
54  
55  
56  
57  
58  
59  
60